PHYSICAL REVIEW A **74**, 051601(R) (2006)

Nonequilibrium coherence dynamics of a soft boson lattice

A. K. Tuchman,[1] C. Orzel,[2] A. Polkovnikov,[3] and M. A. Kasevich[1]
[1]*Physics Department, Stanford University, Stanford, California, 94305, USA*
[2]*Physics and Astronomy Department, Union College, Schenectady, New York 12308, USA*
[3]*Physics Department, Boston University, Boston, Massachusetts 02215, USA*
(Received 28 April 2005; published 15 November 2006)

We study the nonequilibrium evolution of the phase coherence of a Bose-Einstein condensate in a one-dimensional optical lattice as the lattice array is suddenly quenched from a highly-number-squeezed to a superfluid state. We observe slowly damped phase coherence oscillations in the regime of large filling factor (~100 bosons per site) at a frequency proportional to the generalized Josephson frequency.

DOI: 10.1103/PhysRevA.74.051601 PACS number(s): 03.75.Kk, 05.30.Jp, 03.75.Lm

Proposals for Bose-Einstein condensate (BEC) interferometry have demonstrated that number-squeezed states can potentially provide robust sub-shot-noise sensitivity to perturbing interactions [1,2]. The appeal of one recent proposal by Dunningham and Burnett [3] is the current availability of number-squeezed states in an optical lattice [4–6] and the simplicity of the required experimental sequence. In this proposal, an array of number-squeezed states is prepared in a suitably deep optical lattice. The lattice depth is rapidly lowered and the system evolves in the presence of a perturbing potential energy gradient. The lattice depth is then restored to its initial value. A final interferometric measurement of array phase coherence is used to characterize the perturbation. This sequence is analogous to sub-shot-noise optical interferometry using Fock states as inputs to a Mach-Zehnder interferometer [1].

Unlike the optical case, however, this proposal is complicated by both a strong nonlinearity due to the BEC mean-field interaction and multiple interfering modes. In this work, we examine the influence of these factors on coherence dynamics in an optical lattice. We study the phase coherence evolution of highly squeezed number states in response to a sudden reduction in the lattice depth. This sequence induces on-site phase variance oscillations as the quantum state evolves, yielding coherence restoration. We observe these oscillations in the dynamic evolution of interference contrast. To our knowledge, this work is the first to characterize the time scale for coherence restoration in the large-filling-factor regime.

For our experimental parameters (many atoms and lattice sites), exact solutions of the many-body equations of motion are unavailable due to the system's exponentially large Hilbert space. Furthermore, traditional approximations fail in their ability to model the initial state [7]. Density matrix renormalization group techniques have recently been used to study nonequilibrium dynamics of boson lattices with low filling factors [8], but they are difficult to extend to large filling factors. Thus, analysis of this dynamic evolution in an optical lattice is an interesting problem in its own right.

The Bose-Hubbard Hamiltonian accurately describes the atom-lattice system [9,10]. Written in terms of single-particle creation and annihilation operators $(\hat{a}_i^\dagger, \hat{a}_i)$,

$$H = -\gamma \sum_{\langle i,j \rangle} \hat{a}_i^\dagger \hat{a}_j + (g/2) \sum_i \beta_i \hat{a}_i^\dagger \hat{a}_i^\dagger \hat{a}_i \hat{a}_i + \sum_i V_i \hat{a}_i^\dagger \hat{a}_i, \quad (1)$$

where the subscripts index the lowest vibrational mode of each lattice site. Here γ is the tunneling rate between adjacent lattice sites, $g\beta_i$ is the mean-field energy due to repulsive interactions between two atoms ($g = 4\pi\hbar^2 a/m$, a is the s-wave scattering length, and m is the atomic mass) [11], N_i is the number of atoms per site, and $V_i = \Omega i^2$ is the external potential due to a harmonic magnetic trap. The importance of quantum fluctuations is determined by the ratio $g\beta_i/N_i\gamma$, where $g\beta_i/N_i\gamma \sim 1$ indicates the superfluid to Mott-insulator (MI) crossover [9,10,12,13]. We characterize global array phase coherence by the quantity $D(t) = \Sigma_{i \neq j} \langle a_j^\dagger a_i \rangle / NM$, where M is the ratio of the total number of atoms N to the number of atoms in the central lattice site [7].

Qualitative understanding of the system dynamics is obtained by solving Eq. (1) for a two-site model. Figure 1(a) plots the evolution of the number distribution after a sudden reduction in lattice depth for parameters similar to our experimental conditions. Figure 1(b) shows the associated phase distribution (the Fourier transform of the number distribution coefficients). For the two-site system, the characteristic oscillation frequency is the generalized Josephson frequency $\sqrt{4N_i g\beta_i \gamma + 4\gamma^2}$ [14,15]. At the first phase revival [$t \sim 6$ ms in Fig. 1(b)], phase variance is sub-Poissonian while number variance is super-Poissonian. In principle, this enables interferometric phase shift measurements below the atom shot-noise limit [2].

We employ the truncated Wigner approximation (TWA) [16,17] to obtain approximate array dynamics for the full lattice system. In the TWA, the quantum-mechanical expectation value of an observable is replaced by a semiclassical ensemble average. Specializing to the lattice system, we consider a set of wave functions ψ_j which evolve according to the semiclassical, discrete Gross-Pitaevskii equation (GPE) [7,18]:

$$i\hbar \partial \psi_j / \partial t = -\gamma(\psi_{j-1} + \psi_{j+1}) + (V_j + g\beta_j |\psi_j|^2)\psi_j. \quad (2)$$

The initial condition $\psi_j(0) = \sqrt{N_j} e^{i\phi_j}$, where the phases ϕ_j are sampled from a uniform distribution of values between 0 and 2π, and N_j are determined from the GPE ground-state solution. We time evolve $\psi_j(0)$ for a large ensemble of random initial phase distributions and, in Monte Carlo

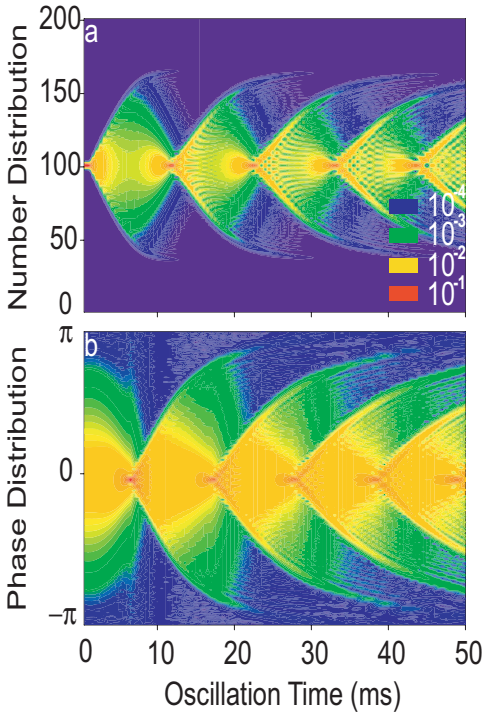

FIG. 1. (Color) (a) Evolution of the number distribution of a two-site system following a 200 ms lattice depth ramp to $65E_R$ and a subsequent diabatic lowering of the depth to $20E_R$, for $N_i=100$ atoms. False color exponential scaling denotes probability of number distribution in one site. (b) Associated phase distribution.

fashion, determine $D(t)$ as the statistical average of these independent GPE simulations [7]. Figure 2 shows an example calculation of $D(t)$ for conditions similar to those used in the experiments described below.

This model is intuitively motivated by the observation that phase is completely undefined for both a Fock state and a superposition of coherent states with random phases [19]. The TWA is accurate for short times and is applied here since the time evolution occurs in the semiclassical superfluid regime [17]. It has been used to analyze the breakdown of adiabaticity for lattice squeezing experiments [4] and to study damping of dipolar motion [20,21]. The TWA results

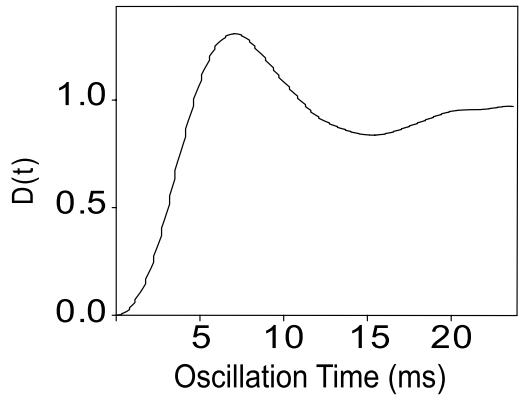

FIG. 2. TWA simulation of $D(t)$ for a final lattice depth of $32E_R$.

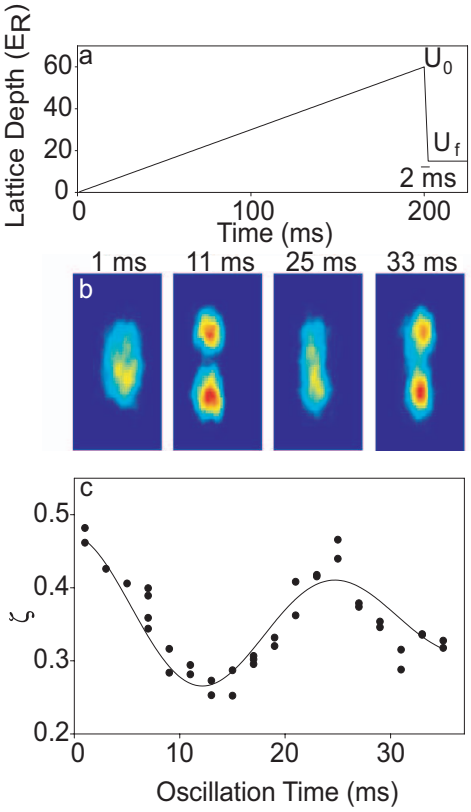

FIG. 3. (Color) (a) Experimental sequence for the lattice depth ramp. The lattice is ramped to a peak value U_0, with corresponding reduced number fluctuations, and then rapidly decreased to U_f. (b) Absorption images of the atom density profile for indicated hold times. (c) Phase variance oscillation with $U_0=63E_R$, $U_f=16.6E_R$, and $\Omega/\hbar=2\pi\times0.67$ Hz.

are consistent with an earlier phonon interpretation of BEC lattice dynamics [22].

The apparatus is described in Ref. [4]. ^{87}Rb atoms are evaporatively cooled in a time-orbiting potential, producing nearly pure condensates ($T/T_c<0.3$) with 3×10^3 atoms in the $F=2, m_F=2$ state. After adiabatically relaxing the confining harmonic potential, the BEC is loaded into a vertically oriented one-dimensional optical lattice. The lattice uses a retroreflected $\lambda=840$ nm laser beam focused to a 50 μm $1/e$ intensity radius at the point of overlap with the BEC. This provides strong transverse confinement and periodic confinement along the propagation axis. At a well depth of $U=63E_R$ ($E_R/\hbar=\hbar k^2/2m\sim2\pi\times3.2$ kHz, $k=2\pi/\lambda$), the transverse oscillation frequency is 150 Hz, significantly larger than the 11 Hz magnetic trap radial frequency [23].

We load the atoms into the lattice by linearly increasing the lattice depth to U_0 in 200 ms [Fig. 3(a)]. The 200 ms ramp speed is slow enough that on-site number fluctuations are substantially suppressed by the end of the ramp despite imperfect adiabaticity [4,6,22,24]. At $U_0=63E_R$, we infer $\gamma/\hbar=2\pi\times0.019$ Hz, $N_0=90$, and $g\beta_0/N_0\gamma=2$ for the central lattice site ($i=0$). We then lower the depth (in 2 ms) to a final level U_f with a corresponding superfluid groundstate. U_f ranges from $12E_R$ to $32E_R$, with $1\leqslant g\beta_0/2\pi\hbar\leqslant2$ Hz and $42\geqslant\gamma/2\pi\hbar\geqslant1$ Hz. The time scale for lowering the poten-

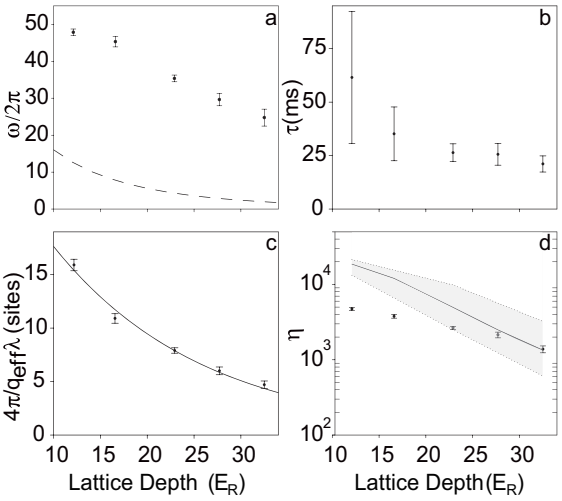

FIG. 4. (Color online) (a) Oscillation frequency as a function of lattice depth. Dashed line shows the calculated quadrupole mode excitation spectrum using the GPE. (b) Damping coefficient τ vs lattice depth. (c) $4\pi/q_{\text{eff}}\lambda$ lattice sites vs lattice depth. Solid line is exponential fit to data. (d) Initial curvature η of the phase variance oscillation vs lattice depth. Solid line depicts results of the TWA. Shaded region reflects experimental uncertainty.

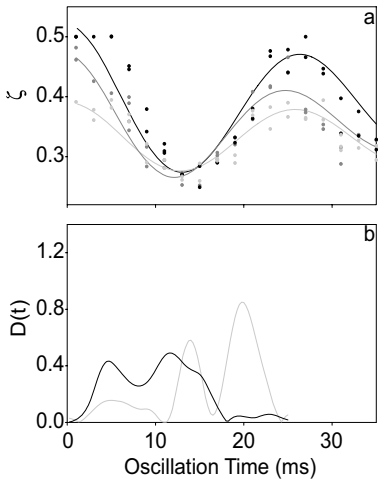

FIG. 5. (a) Phase variance oscillations for $U_0=80E_R$ (black), $63E_R$ (dark gray) and $50E_R$ (light gray) with $U_f=17E_R$. (b) GPE simulation of $D(t)$ for lattice sequence in Fig. 3 for $U_0=80E_R$ (black) and $50E_R$ (gray).

tial is fast compared to the characteristic time scale for adiabatic evolution of the many-body ground state but slow with respect to the oscillation frequency of individual wells.

We stroboscopically follow the array phase coherence evolution after lowering the lattice depth to U_f by holding the atoms in the lattice before releasing them and observing their de Broglie wave interference. We reduce the strength of the confining magnetic potential (in 300 μs) and hold the atoms in the lattice+gravity potential for a time sufficient to introduce a $\pi/2$ phase shift between adjacent sites before extinguishing the lattice light. This $\pi/2$ phase shift produces a two-peaked interference pattern when long-range array phase coherence exists.

Figure 3(b) displays a series of absorption images of the atomic density profile as the quantum state evolves. We characterize the interference patterns through the contrast parameter ζ, defined as the width of a single peak to the separation between the peaks. Large ζ indicates loss of interference contrast. ζ is obtained by fitting the data to two displaced Gaussians with equal widths. Figure 3(c) shows the oscillatory response of ζ as a function of hold time. Coherence restoration is observed, indicating the evolution of relative number fluctuations. Although it is tempting to identify the state associated with the maximum return of contrast with a phase-squeezed state (as in Fig. 1), our observation cannot distinguish between this state and other states which also support relative phase coherence. Future work will be geared toward an explicit characterization of the high-order coherence properties associated with the state as it dynamically evolves.

In order to gain further insight into the mechanism underlying the contrast oscillations, we study the lattice dynamics as a function of U_f. The oscillatory response is analyzed by fitting the functional form $A\exp(-t/\tau)\cos(\omega t)$ to the data (τ is the characteristic damping time and ω the characteristic frequency). As U_f is increased, a monotonic decrease in both ω [Fig. 4(a)] and τ [Fig. 4(b)] is observed. For reference, we also plot the characteristic frequencies associated with the GPE-predicted quadrupole breathing mode in Fig. 4(a) [25].

The oscillation frequencies can be interpreted in terms of effective phonon wave vectors q_{eff}. We infer q_{eff} from the phonon dispersion relation for a uniform lattice [26]:

$$\hbar\omega_q = \sqrt{4\gamma\sin^2(q\lambda/4)[2N_i g\beta + 4\gamma\sin^2(q\lambda/4)]}. \qquad (3)$$

For each observed frequency ω, we find the corresponding excitation wave vector q_{eff} such that the lowest-lying phonon excitation frequency ω_q is equal to ω [Fig. 4(c)]. For sufficiently large U_f, ω corresponds to a short-wavelength excitation and is proportional to the generalized Josephson frequency. For our parameters, this is much faster than the single-particle tunneling frequency which has been previously observed to determine the time scale for the onset of coherence in a lattice system with low filling factor [5]. It is interesting to note that an exponential fit to the data extrapolates to $4\pi/q_{\text{eff}}\lambda=1$ site at $55E_R$, a lattice depth close to the MI crossover.

In order to make contact with the predictions of TWA theory, we consider the short-time dynamics associated with the onset of coherence. We characterize the contrast oscillations through their initial curvature η. To compare with theory [Fig. 4(d)], we normalize the oscillation amplitudes of $D(t)$ (Fig. 2) and $\zeta(t)$ [Fig. 3(c)] to those values associated with a return to full coherence [27]. We find that the TWA effectively captures the short-time dynamics over a substantial range of U_f.

Lattice depths used for the initial state preparation are deep enough that this step cannot be considered fully adiabatic. Therefore, the state at U_0 is likely described by a highly squeezed number state with some additional phonon excitations [22,24]. We place bounds on the influence of nonadiabatic behavior in two ways. First, we use the two-site model to simulate the state preparation ramp for our experi-

mental conditions. In all cases, number fluctuations of the initial state are approximately one atom per lattice site. Second, we experimentally investigate the dependence of the oscillations on U_0, keeping U_f and the ramp time fixed [Fig. 5(a)]. Within the limits of our experimental uncertainties, the observed ω is independent of U_0 for $50E_R < U_0 < 80E_R$. Intuitively, we understand this invariant behavior by noting that for the deep lattices used, the dominant nonadiabatic dephasing mechanism is a homogeneous mechanism whose origin is the mean-field-induced decoupling of the relative phases of the Fock-state components associated with the quantum state at each lattice site [6,28]. In the TWA picture, such a state is modeled by randomly choosing N_i and ϕ_i at each lattice site. Since the variance in N_i is small, this amounts to a negligible correction for the dynamics.

We note that the observed independence of dynamics on U_0 rules out a semiclassical (GPE) mechanism whose origin is remnant phase coherence between lattice sites introduced by nonadiabaticity during state preparation. Although this inhomogeneous mechanism is likely masked by the homogeneous mechanism described above, we assess its possible relevance through GPE numerical solutions. Figure 5(b) shows solutions obtained by integrating Eqs. (2) over the experimental sequence including the state preparation lattice ramp, with $\phi_j=0$ as the initial condition. In this case, the loss of global phase coherence following state preparation is driven by site-to-site nonuniformities in the array chemical potential. In contrast to our observations and the TWA, these solutions show a strong dependence on U_0.

In summary, we have shown that the TWA accurately models the short time non-equilibrium dynamics for the soft boson lattice system. Future work will investigate lattice implementations of sub-shot-noise interferometry.

We acknowledge A. Smerzi, S. Sachdev, and S. Girvin for helpful discussions and M. Fenselau and S. Dettmer for technical assistance. This work was funded by grants from DARPA, NSF, and ARO/MURI. A.P. acknowledges NSF Grants No. DMR-0231631 and DMR-0213805. A.K.T. was supported by the IC and NGA.

[1] M. J. Holland and K. Burnett, Phys. Rev. Lett. **71**, 1355 (1993).
[2] P. Bouyer and M. A. Kasevich, Phys. Rev. A **56**, R1083 (1997).
[3] J. A. Dunningham and K. Burnett, Phys. Rev. A **70**, 033601 (2004).
[4] C. Orzel *et al.*, Science **291**, 2386 (2001).
[5] M. Greiner *et al.*, Nature (London) **415**, 39 (2002).
[6] W. Li *et al.*, e-print quant-ph/0609009 (2006).
[7] A. Polkovnikov *et al.*, Phys. Rev. A **66**, 053607 (2002).
[8] S. R. Clark and D. Jaksch, Phys. Rev. A **70**, 043612 (2004); see also, G. Vidal, Phys. Rev. Lett. **93**, 040502 (2004).
[9] M. P. A. Fisher *et al.*, Phys. Rev. B **40**, 546 (1989).
[10] D. Jaksch *et al.*, Phys. Rev. Lett. **81**, 3108 (1998).
[11] In the Thomas-Fermi regime in the radial direction, $g\beta_i = (m\omega_{z0}\omega_\perp^4\hbar^3a^2/2\pi N_i^2)^{1/4}$ with $\omega_\perp$ and ω_{z0} the radial and longitudinal oscillation frequencies characteristic of an individual lattice site.
[12] C. Kollath *et al.*, Phys. Rev. A **69**, 031601(R) (2004).
[13] D. van Oosten *et al.*, Phys. Rev. A **67**, 033606 (2003).
[14] A. Smerzi *et al.*, Phys. Rev. Lett. **79**, 4950 (1997).
[15] G. Paraoanu *et al.*, J. Phys. B **34**, 4689 (2001).
[16] M. J. Steel *et al.*, Phys. Rev. A **58**, 4824 (1998).
[17] A. Polkovnikov, Phys. Rev. A **68**, 033609 (2003); Phys. Rev. A **68**, 053604 (2003).
[18] A. Trombettoni and A. Smerz, Phys. Rev. Lett. **86**, 2353 (2001).
[19] The Wigner transform of the initial Fock state does have a nontrivial oscillatory behavior in the distribution of the number N_j. However, when $N_j \gg 1$, its influence on the phase coherence oscillations is negligible [17].
[20] A. Polkovnikov and D. N. Wang, Phys. Rev. Lett. **93**, 070401 (2004).
[21] L. Isella and J. Ruostekoski, Phys. Rev. A **72**, 011601(R) (2005).
[22] J. Javanainen, Phys. Rev. A **60**, 4902 (1999).
[23] Lattice depth is calibrated with ~20% error by measuring atom loss due to resonant heating. The uncertainty in our atom number is 20%.
[24] J. Ruostekoski and L. Isella, Phys. Rev. Lett. **95**, 110403 (2005); e-print cond-mat/0608634.
[25] M. Kramer *et al.*, Phys. Rev. Lett. **88**, 180404 (2002).
[26] K. Burnett *et al.*, J. Phys. B **35**, 1671 (2002).
[27] The maximum amplitude for $\zeta(t)$ oscillations is 0.135 (for $U_f < 15E_R$). Corresponding amplitude for $D(t)$ is 0.65.
[28] A. Imamoglu *et al.*, Phys. Rev. Lett. **78**, 2511 (1997).